Composites: Part B xxx (2012) xxx–xxx

Contents lists available at SciVerse ScienceDirect

Composites: Part B

journal homepage: www.elsevier.com/locate/compositesb

Non-linear pre-buckling behavior of shear deformable thin-walled composite beams with open cross-section

Geminiano Mancusi *, Luciano Feo

Department of Civil Engineering, University of Salerno, 84084 Fisciano, Italy

ARTICLE INFO

Article history:
Received 25 October 2012
Received in revised form 6 November 2012
Accepted 6 November 2012
Available online xxxx

Keywords:
A. Polymer–matrix composites (PMCs)
B. Buckling
C. Finite element analysis (FEA)
E. Pultrusion

ABSTRACT

A kinematic model is presented for thin-walled composite beams able to account for axial force, bending, torsion and warping. Shear deformations on the mid-surface are considered and modeled by means of a polynomial approximation. For this scope appropriate shape functions on the curvilinear abscissa along the cross-section mid-line are introduced.

Small strains and moderate rotations are considered over the pre-buckling range.

The model allows to predict the static non-linear behavior and the critical loads of composite pultruded beams.

A finite element approximation is derived from a variational approach. Some numerical results are also presented revealing the importance of the shear terms on the mechanical response and their effect on the stability of pultruded composite members.

1. Introduction

Thin-walled composite beams with open cross-section obtained by the pultrusion process have been increasingly used in civil engineering. Nevertheless, due to the relevance of shear deformability, the practical use of composite profiles still conflicts with the serviceability requirements related to the stiffness demand for civil applications. Composite materials offer many advantages over traditional materials, such as light weight and high resistance against corrosion, but also require a rigorous evaluation of their structural performance from many points of view which are related to the instantaneous and long-term behavior, the influence of the shear deformability as well as the influence of the second order terms over the pre-buckling behavior.

Limiting the study within the linear-elastic field, the behavior of thin-walled composite beams with open cross-section can be modeled by extending the theory of Vlasov [1] to account for anisotropy [2,3] and shear deformations on the mid-surface [4–8]. However, since both the fibers and resin of a composite beam can sustain large elongations up to rupture, in most circumstances the failure is due to elastic buckling with the load carrying capacity being directly related to the critical buckling load.

Specific studies available in literature [9–22] deal with the Euler and torsional buckling of thin-walled columns as well as the lateral buckling, which, in particular, shows a certain complexity since structures may exhibit large or moderately large deflections and rotations over the pre-buckling range.

Within this context the present paper deals with the formulation of a moderate rotation theory of thin-walled composite beams. The kinematic model is assumed to be characterized by small strains at the longitudinal axis, small warping strains and moderately large rigid-body rotations of the cross-sections As discussed elsewhere [23–26], under certain restrictions on the diameter of the cross-section, such assumptions ensure small strains and moderate rotations within the whole beam.

Shear deformability is modeled according to the approach proposed in [6,7] by using a refined polynomial approximation of the angular sliding on the mid-surface of the thin-walled beam.

A finite element approximation is derived via a variational approach. Numerical algorithms [27] are adopted to follow an arbitrary equilibrium path of the beam as well as compute stability points. Finally, some numerical results are also given in order to highlight the non-linear pre-buckling behavior of pultruded composite beams.

* Corresponding author.
E-mail addresses: g.mancusi@unisa.it (G. Mancusi), l.feo@unisa.it (L. Feo).

1359-8368/$ - see front matter © 2012 Elsevier Ltd. All rights reserved.
http://dx.doi.org/10.1016/j.compositesb.2012.11.003

2. Notations

A list of the main relevant symbols is presented.

$\{\Omega,\mathbf{i},\mathbf{j},\mathbf{k}\}$	Global reference system
$\{\overline{\mathbf{P}},\mathbf{n},\mathbf{t},\mathbf{k}\}$	Local reference system
L	Length of the beam axis
b	Thickness of the walled beam
$\Sigma_{(1)},\Sigma_{(2)}$	Ends of the beam
Σ	Generic cross-section
A	Cross-section area
λ	Mid-line of Σ
l	Length of λ
ρ	In-plane curvature radius of λ
$\mathbf{O}$	Intersection between the $\mathbf{k}$ axis and the plane of Σ
$\mathbf{C}$	Arbitrary fixed pole
$\mathbf{P}$	Generic point of the beam
$\mathbf{x}$	Position vector of the generic point
$\overline{\mathbf{P}}$	Projection of $\mathbf{P}$ on the mid-surface
$\tilde{x}$	Oriented distance from $\overline{\mathbf{P}}$ to $\mathbf{P}$
s	Curvilinear coordinate along λ
$\mathbf{M}$	Origin of s
$\mathbf{u}$	Displacement field
$\tilde{\zeta}$	Warping function
$\mathbf{H}$	Displacement gradient
$\boldsymbol{\varepsilon}$	Symmetric part of $\mathbf{H}$
e	Norm of $\boldsymbol{\varepsilon}$
$\mathbf{E}$	Green strain tensor
δL_i	Virtual work done by internal stresses
δL_e	Virtual work done by external loads
$\mathbf{b}$	External force for unit volume
$\mathbf{p}$	External force for unit surface acting on the boundary of the beam

3. Mechanical model

In this section are introduced the main features of a mechanical model proposed for the non-linear analysis of pultruded composite beams. They relate to many assumptions concerning the geometric and mechanical smallness as well as the constitutive relationships.

3.1. Geometric smallness

The geometry of the beam under consideration is given in Figs. 1 and 2. In particular, the global reference system $\{\Omega,\mathbf{i},\mathbf{j},\mathbf{k}\}$ has been oriented by aligning the unit vector $\mathbf{k}$ with the longitudinal axis of the beam, while the reference systems $\{\overline{\mathbf{P}},\mathbf{n},\mathbf{t},\mathbf{k}\}$ have been introduced with the local origin $\overline{\mathbf{P}}$ lying on the mid-surface of the beam. It results:

$$\mathbf{n}=\frac{\mathrm{d}y}{\mathrm{d}s}\mathbf{i}-\frac{\mathrm{d}x}{\mathrm{d}s}\mathbf{j}\qquad \mathbf{t}=\frac{\mathrm{d}x}{\mathrm{d}s}\mathbf{i}+\frac{\mathrm{d}y}{\mathrm{d}s}\mathbf{j} \tag{1.a, b}$$

$$\frac{\mathrm{d}\mathbf{n}}{\mathrm{d}s}=-\frac{1}{\rho}\mathbf{t}\qquad \frac{\mathrm{d}\mathbf{t}}{\mathrm{d}s}=\frac{1}{\rho}\mathbf{n} \tag{2.a, b}$$

with $x = x(s)$ and $y = y(s)$ being the parametric equations of the mid-line λ and ρ the following quantity:

$$\rho=\sqrt{\left(\frac{\mathrm{d}^2x}{\mathrm{d}s^2}\right)^2+\left(\frac{\mathrm{d}^2y}{\mathrm{d}s^2}\right)^2} \tag{3}$$

From Eqs. (1) and (2), it descends:

$$\frac{\mathrm{d}^2x}{\mathrm{d}s^2}=\frac{\mathrm{d}\mathbf{t}}{\mathrm{d}s}\cdot\mathbf{i}=\frac{1}{\rho}\mathbf{n}\cdot\mathbf{i}=\frac{1}{\rho}\frac{\mathrm{d}y}{\mathrm{d}s} \tag{4.a}$$

$$\frac{\mathrm{d}^2y}{\mathrm{d}s^2}=\frac{\mathrm{d}\mathbf{t}}{\mathrm{d}s}\cdot\mathbf{j}=\frac{1}{\rho}\mathbf{n}\cdot\mathbf{j}=-\frac{1}{\rho}\frac{\mathrm{d}x}{\mathrm{d}s} \tag{4.b}$$

Due to the hypothesis of small thickness of the walled beam, the following relationships are supposed to be satisfied:

$$\frac{b}{l}\ll 1\qquad \frac{b}{\rho}\ll 1 \tag{5.a, b}$$

being l the length of the mid-line λ.

From Eqs. (4) and (5), finally, it results:

$$b\frac{\mathrm{d}^2x}{\mathrm{d}s^2}\ll 1\qquad b\frac{\mathrm{d}^2y}{\mathrm{d}s^2}\ll 1 \tag{6.a, b}$$

3.2. Basic kinematic assumptions

The position of a generic point $\mathbf{P}$ of the beam is:

$$\mathbf{x}(\mathbf{P})=\mathbf{x}(\overline{\mathbf{P}})+\tilde{x}\mathbf{n}=x\mathbf{i}+y\mathbf{j}+z\mathbf{k}+\tilde{x}\mathbf{n} \tag{7}$$

where $\overline{\mathbf{P}}$ is the normal projection of $\mathbf{P}$ on the mid-surface of the beam; x, y and z are the coordinates of $\overline{\mathbf{P}}$ referred to the global system; $\tilde{x}$ denotes the oriented distance measured from $\overline{\mathbf{P}}$ to $\mathbf{P}$ (Fig. 2).

Furthermore, the projections along $\mathbf{n}$ and $\mathbf{t}$ of the distance vector from an arbitrary fixed point $\mathbf{C}$ to $\mathbf{P}$, are:

$$[\mathbf{x}(\mathbf{P})-\mathbf{x}(\mathbf{C})]\cdot\mathbf{n}=r+\tilde{x}\qquad [\mathbf{x}(\mathbf{P})-\mathbf{x}(\mathbf{C})]\cdot\mathbf{t}=p \tag{8.a, b}$$

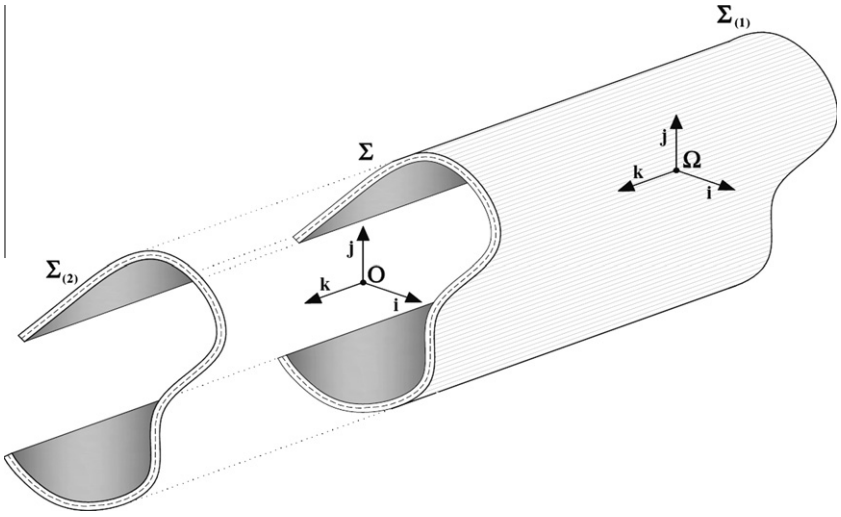

Fig. 1. Thin-walled beam configuration.

Please cite this article in press as: Mancusi G, Feo L. Non-linear pre-buckling behavior of shear deformable thin-walled composite beams with open cross-section. Composites: Part B (2012), http://dx.doi.org/10.1016/j.compositesb.2012.11.003

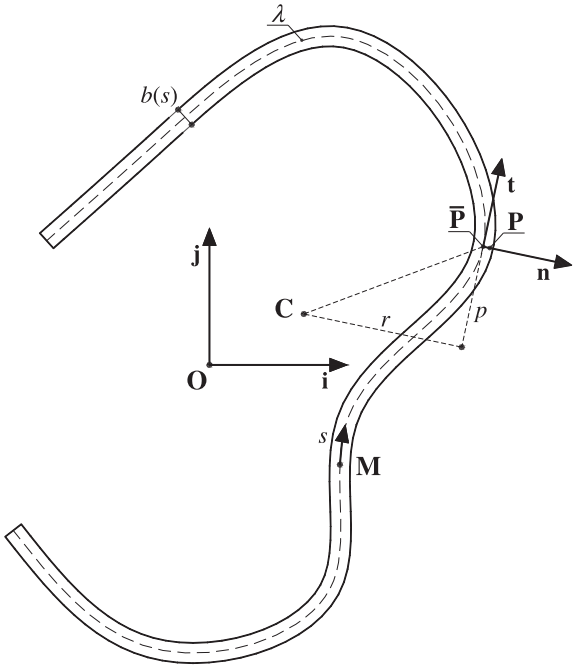

Fig. 2. Generic cross-section Σ.

where

$$r = (x - x_c)\frac{dy}{ds} - (y - y_c)\frac{dx}{ds}$$
$$p = (x - x_c)\frac{dx}{ds} + (y - y_c)\frac{dy}{ds} \quad (9.a, b)$$

The kinematics of the thin-walled beam has been modeled by assuming that the generic cross-section preserves itself undeformed and exhibits rigid-body rotations accompanied by warping displacements out of its plane:

$$\mathbf{u}(\mathbf{x}) = \mathbf{u}(\mathbf{x}_c) + (\mathbf{R} - \mathbf{I})(\mathbf{x} - \mathbf{x}_c) + \hat{\zeta}(\mathbf{x})\mathbf{k} \quad (10)$$

In Eq. (10) the symbols have the following meanings:

- $\mathbf{u} = [\xi, \eta, \zeta]^T$ denotes the displacement field vector with ξ, η and ζ indicating, in order, the displacement components along the axes x, y and z;
- $\mathbf{x}$ is the position of a generic point **P** of the beam;
- $\mathbf{x}_c = [x_c, y_c, z]^T$ is the position of the point **C** relative to the generic cross-section at a distance z from Ω;
- $\mathbf{I}$ is the identity tensor;
- $\mathbf{R}$ is a rotation tensor ($\mathbf{R}^T\mathbf{R} = \mathbf{R}\mathbf{R}^T = \mathbf{I}$);
- $\hat{\zeta}(\mathbf{x})$ is the warping function.

According to the results presented in [26], the tensor $\mathbf{R}$ can be expressed as follows:

$$\mathbf{R} = \mathbf{I} + \mathbf{\Psi} \quad (11)$$

where

$$\mathbf{\Psi} = \mathbf{\Phi} + \frac{1}{2!}\mathbf{\Phi}^2 + \frac{1}{3!}\mathbf{\Phi}^3 + \cdots \quad (12)$$

being $\mathbf{\Phi}$ a skew tensor. From Eqs. (11) and (12) it is possible to write the displacement field components in the form:

$$\xi = \xi_c + \Psi_{11}(x - x_c) + \Psi_{12}(y - y_c) \quad (13.a)$$
$$\eta = \eta_c + \Psi_{21}(x - x_c) + \Psi_{22}(y - y_c) \quad (13.b)$$
$$\zeta = \zeta_c + \Psi_{31}(x - x_c) + \Psi_{32}(y - y_c) + \hat{\zeta} \quad (13.c)$$

where ξ_c, η_c and ζ_c indicate, in order, the displacement components along the axes x, y and z of the point **C**.

3.3. Strain smallness

From Eq. (13), it is easy to obtain the following components of the displacement gradient $\mathbf{H} = \nabla\mathbf{u}$, expressed with reference to the global coordinates.

$$H_{11} = \Psi_{11} \quad (14.a)$$
$$H_{12} = \Psi_{12} \quad (14.b)$$
$$H_{13} = \xi_c' + \Psi_{11}'(x - x_c) + \Psi_{12}'(y - y_c) \quad (14.c)$$
$$H_{21} = \Psi_{21} \quad (14.d)$$
$$H_{22} = \Psi_{22} \quad (14.e)$$
$$H_{23} = \eta_c' + \Psi_{21}'(x - x_c) + \Psi_{22}'(y - y_c) \quad (14.f)$$
$$H_{31} = \Psi_{31} + \frac{\partial\hat{\zeta}}{\partial x} \quad (14.g)$$
$$H_{32} = \Psi_{32} + \frac{\partial\hat{\zeta}}{\partial y} \quad (14.h)$$
$$H_{33} = \zeta_c' + \Psi_{31}'(x - x_c) + \Psi_{32}'(y - y_c) + \frac{\partial\hat{\zeta}}{\partial z} \quad (14.i)$$

On the other hand, its symmetric part $\boldsymbol{\varepsilon} = 1/2(\mathbf{H} + \mathbf{H}^T)$ is given by:

$$\varepsilon_{11} = \Psi_{11} \quad (15.a)$$
$$\varepsilon_{22} = \Psi_{22} \quad (15.b)$$
$$\varepsilon_{33} = \zeta_c' + \Psi_{31}'(x - x_c) + \Psi_{32}'(y - y_c) + \frac{\partial\hat{\zeta}}{\partial z} \quad (15.c)$$
$$\varepsilon_{12} = \frac{1}{2}(\Psi_{12} + \Psi_{21}) \quad (15.d)$$
$$\varepsilon_{13} = \frac{1}{2}\left(\xi_c' + \Psi_{11}'(x - x_c) + \Psi_{12}'(y - y_c) + \Psi_{31} + \frac{\partial\hat{\zeta}}{\partial x}\right) \quad (15.e)$$
$$\varepsilon_{23} = \frac{1}{2}\left(\eta_c' + \Psi_{21}'(x - x_c) + \Psi_{22}'(y - y_c) + \Psi_{32} + \frac{\partial\hat{\zeta}}{\partial y}\right) \quad (15.f)$$

As discussed in [27], the following smallness hypotheses are pivotal:

$$e \ll 1 \quad (16.a)$$
$$\mathbf{\Phi} = \mathbf{O}(e^{1/2}) \quad (16.b)$$
$$\nabla\hat{\zeta} = O(e) \quad (16.c)$$
$$\mathbf{\Phi}' = \mathbf{O}(e^{1/2}) \quad (16.d)$$
$$\boldsymbol{\varepsilon}'(x_c, y_c, z) = \mathbf{O}(e) \quad (16.e)$$

with

$$e = \sup_{z\in[0,L]}\|\boldsymbol{\varepsilon}(x_c, y_c, z)\| \quad (17)$$

All the above assumptions imply that the deformation of the beam results in small strains and moderate rotations [25], according to the following representation of the tensor $\mathbf{\Psi}$:

$$\mathbf{\Psi} = \mathbf{\Phi} + \frac{1}{2}\mathbf{\Phi}^2 + \mathbf{O}(e^{3/2}) \cong \begin{bmatrix} 0 & -\varphi_z & \varphi_y \\ \varphi_z & 0 & -\varphi_x \\ -\varphi_y & \varphi_x & 0 \end{bmatrix} - \frac{1}{2}\begin{bmatrix} (\varphi_y^2 + \varphi_z^2) & -\varphi_x\varphi_y & -\varphi_x\varphi_z \\ -\varphi_x\varphi_y & (\varphi_x^2 + \varphi_z^2) & -\varphi_y\varphi_z \\ -\varphi_x\varphi_z & -\varphi_y\varphi_z & (\varphi_x^2 + \varphi_y^2) \end{bmatrix} \quad (18)$$

Furthermore, it results [27]:

$$\varphi_x = -\eta_c' + O(e) \qquad \varphi_x' = -\eta_c'' + O(e) \quad (19.a, b)$$

Please cite this article in press as: Mancusi G, Feo L. Non-linear pre-buckling behavior of shear deformable thin-walled composite beams with open cross-section. Composites: Part B (2012), http://dx.doi.org/10.1016/j.compositesb.2012.11.003

$$\varphi_y = \xi_c' + O(e) \qquad \varphi_y' = \xi_c'' + O(e) \tag{19.c, d}$$

$$\zeta_c' = O(e) \qquad \zeta_c'' + \left(\left.\frac{\partial \zeta}{\partial z}\right|_{\mathbf{x}=\mathbf{x}_c}\right)' = O(e) \tag{19.e, f}$$

As a consequence, the new form of the displacement field is:

$$\xi = \xi_c - \frac{1}{2}\left(\varphi_y^2 + \varphi_z^2\right)\Delta x + \left(-\varphi_z + \frac{1}{2}\varphi_x\varphi_y\right)\Delta y \tag{20.a}$$

$$\eta = \eta_c + \left(\varphi_z + \frac{1}{2}\varphi_x\varphi_y\right)\Delta x - \frac{1}{2}\left(\varphi_x^2 + \varphi_z^2\right)\Delta y, \tag{20.b}$$

$$\zeta = \zeta_c + \left(-\varphi_y + \frac{1}{2}\varphi_x\varphi_z\right)\Delta x + \left(\varphi_x + \frac{1}{2}\varphi_y\varphi_z\right)\Delta y + \hat{\zeta} \tag{20.c}$$

where

$$\Delta x = \left(x - x_c + \frac{dy}{ds}\tilde{x}\right)$$

$$\Delta y = \left(y - y_c - \frac{dx}{ds}\tilde{x}\right) \tag{21.a, b}$$

By means of Eq. (20), it is possible to up-date the components of $\mathbf{H} = \nabla\mathbf{u}$ as follows:

$$H_{11} = \frac{\partial \xi}{\partial x} = -\frac{1}{2}\left(\varphi_y^2 + \varphi_z^2\right) \tag{22.a}$$

$$H_{12} = \frac{\partial \xi}{\partial y} = -\varphi_z + \frac{1}{2}\varphi_x\varphi_y \tag{22.b}$$

$$H_{13} = \frac{\partial \xi}{\partial z} = \xi_c' - \left(\varphi_y\varphi_y' + \varphi_z\varphi_z'\right)\Delta x + \left(-\varphi_z' + \frac{1}{2}\varphi_x\varphi_y' + \frac{1}{2}\varphi_x'\varphi_y\right)\Delta y \tag{22.c}$$

$$H_{21} = \frac{\partial \eta}{\partial x} = \varphi_z + \frac{1}{2}\varphi_x\varphi_y \tag{22.d}$$

$$H_{22} = \frac{\partial \eta}{\partial y} = -\frac{1}{2}\left(\varphi_x^2 + \varphi_z^2\right) \tag{22.e}$$

$$H_{23} = \frac{\partial \eta}{\partial z} = \eta_c' + \left(\varphi_z' + \frac{1}{2}\varphi_x\varphi_y' + \frac{1}{2}\varphi_x'\varphi_y\right)\Delta x - \left(\varphi_x\varphi_x' + \varphi_z\varphi_z'\right)\Delta y \tag{22.f}$$

$$H_{31} = \frac{\partial \zeta}{\partial x} = -\varphi_y + \frac{1}{2}\varphi_x\varphi_z + \frac{\partial \hat{\zeta}}{\partial x} \tag{22.g}$$

$$H_{32} = \frac{\partial \zeta}{\partial y} = \varphi_x + \frac{1}{2}\varphi_y\varphi_z + \frac{\partial \hat{\zeta}}{\partial y} \tag{22.h}$$

$$H_{33} = \frac{\partial \zeta}{\partial z} = \zeta_c' + \left(-\varphi_y' + \frac{1}{2}\varphi_x\varphi_z' + \frac{1}{2}\varphi_x'\varphi_z\right)\Delta x + \left(\varphi_x' + \frac{1}{2}\varphi_y\varphi_z' + \frac{1}{2}\varphi_y'\varphi_z\right)\Delta y + \frac{\partial \hat{\zeta}}{\partial z} \tag{22.i}$$

3.4. Integration of the warping function

With reference to the global axes it is easy to verify that the Green strain tensor assumes the following form (being E_{13}, E_{23} and E_{33} the only non-trivial strain components):

$$\mathbf{E} = \frac{1}{2}\left(\mathbf{H} + \mathbf{H}^T + \mathbf{H}^T\mathbf{H}\right) = \begin{bmatrix} 0 & 0 & E_{13} \\ 0 & 0 & E_{23} \\ E_{13} & E_{23} & E_{33} \end{bmatrix} \tag{23}$$

where

$$E_{13} = \frac{1}{2}\left[\left(\xi_c' - \varphi_y + \frac{1}{2}\varphi_x\varphi_z + \varphi_z\eta_c'\right) + \left(-\varphi_z' + \frac{1}{2}\varphi_x\varphi_y' - \frac{1}{2}\varphi_x'\varphi_y\right)\Delta y + \frac{\partial \hat{\zeta}}{\partial x}\right] \tag{24.a}$$

$$E_{23} = \frac{1}{2}\left[\left(\eta_c' + \varphi_x + \frac{1}{2}\varphi_y\varphi_z - \varphi_z\xi_c'\right) + \left(\varphi_z' - \frac{1}{2}\varphi_x\varphi_y' + \frac{1}{2}\varphi_x'\varphi_y\right)\Delta x + \frac{\partial \hat{\zeta}}{\partial y}\right] \tag{24.b}$$

$$E_{33} = \zeta_c' + \frac{1}{2}\left(\xi_c'\right)^2 + \frac{1}{2}\left(\eta_c'\right)^2 + \frac{\partial \hat{\zeta}}{\partial z} + \left(-\varphi_y' + \frac{1}{2}\varphi_x\varphi_z' + \frac{1}{2}\varphi_x'\varphi_z + \varphi_z'\eta_c'\right)\Delta x + \left(\varphi_x' + \frac{1}{2}\varphi_y\varphi_z' + \frac{1}{2}\varphi_y'\varphi_z - \varphi_z'\xi_c'\right)\Delta y + \frac{1}{2}\left[\left(\varphi_y'\right)^2 + \left(\varphi_z'\right)^2\right](\Delta x)^2 + \frac{1}{2}\left[\left(\varphi_x'\right)^2 + \left(\varphi_z'\right)^2\right](\Delta y)^2 - \varphi_x'\varphi_y'\Delta x\Delta y \tag{24.c}$$

In view of integrating the warping function, it is useful to represent the Green strain tensor as follows:

$$\tilde{\mathbf{E}} = \mathbf{Q}^T\mathbf{E}\mathbf{Q} = \begin{bmatrix} 0 & 0 & E_{nz} \\ 0 & 0 & E_{tz} \\ E_{nz} & E_{tz} & E_{zz} \end{bmatrix} \tag{25}$$

where the symbol "$\sim$" is used to indicate that the strain components have been referred to the local reference system $\{\mathbf{n}, \mathbf{t}, \mathbf{k}\}$. In Eq. (25) the symbol $\mathbf{Q}$ denotes the well-known tensor:

$$\mathbf{Q} = \begin{bmatrix} \frac{dy}{ds} & \frac{dx}{ds} & 0 \\ -\frac{dx}{ds} & \frac{dy}{ds} & 0 \\ 0 & 0 & 1 \end{bmatrix} \tag{26}$$

With reference to the local axes, the strain components E_{nz} and E_{tz} assume the following form:

$$E_{nz} = \frac{1}{2}\left[\left(\xi_c' - \varphi_y + \frac{1}{2}\varphi_x\varphi_z + \varphi_z\eta_c'\right)\frac{dy}{ds} - \left(\eta_c' + \varphi_x + \frac{1}{2}\varphi_y\varphi_z - \varphi_z\xi_c'\right)\frac{dx}{ds} - \left(\varphi_z' - \frac{1}{2}\varphi_x\varphi_y' + \frac{1}{2}\varphi_x'\varphi_y\right)p + \left(\frac{\partial \hat{\zeta}}{\partial x}\frac{dy}{ds} - \frac{\partial \hat{\zeta}}{\partial y}\frac{dx}{ds}\right)\right] \tag{27.a}$$

$$E_{tz} = \frac{1}{2}\left[\left(\xi_c' - \varphi_y + \frac{1}{2}\varphi_x\varphi_z + \varphi_z\eta_c'\right)\frac{dx}{ds} + \left(\eta_c' + \varphi_x + \frac{1}{2}\varphi_y\varphi_z - \varphi_z\xi_c'\right)\frac{dy}{ds} + \left(\varphi_z' - \frac{1}{2}\varphi_x\varphi_y' + \frac{1}{2}\varphi_x'\varphi_y\right)(r + \tilde{x}) + \left(\frac{\partial \hat{\zeta}}{\partial x}\frac{dx}{ds} + \frac{\partial \hat{\zeta}}{\partial y}\frac{dy}{ds}\right)\right] \tag{27.b}$$

Due the small thickness of the walled beam, it can be assumed $E_{nz} = 0$, thus implying that the derivative of the warping function $\hat{\zeta}$ with respect to $\mathbf{n}$ can be written as:

$$\frac{\partial \hat{\zeta}}{\partial n} = \frac{\partial \hat{\zeta}}{\partial x}\frac{dy}{ds} - \frac{\partial \hat{\zeta}}{\partial y}\frac{dx}{ds} = -\left(\xi_c' - \varphi_y + \frac{1}{2}\varphi_x\varphi_z + \varphi_z\eta_c'\right)\frac{dy}{ds} + \left(\eta_c' + \varphi_x + \frac{1}{2}\varphi_y\varphi_z - \varphi_z\xi_c'\right)\frac{dx}{ds} + \left(\varphi_z' - \frac{1}{2}\varphi_x\varphi_y' + \frac{1}{2}\varphi_x'\varphi_y\right)p \tag{28}$$

Please cite this article in press as: Mancusi G, Feo L. Non-linear pre-buckling behavior of shear deformable thin-walled composite beams with open cross-section. Composites: Part B (2012), http://dx.doi.org/10.1016/j.compositesb.2012.11.003

By integrating Eq. (28), it results:

$$\hat{\zeta}=\hat{\zeta}|_{\tilde{x}=0}=-\left(\xi_c'-\varphi_y+\tfrac{1}{2}\varphi_x\varphi_z+\varphi_z\eta_c'\right)\tfrac{dy}{ds}\tilde{x}+\left(\eta_c'+\varphi_x+\tfrac{1}{2}\varphi_y\varphi_z-\varphi_z\xi_c'\right)\tfrac{dx}{ds}\tilde{x}+\left(\varphi_z'-\tfrac{1}{2}\varphi_x\varphi_y'+\tfrac{1}{2}\varphi_x'\varphi_y\right)p\tilde{x} \tag{29}$$

where $\hat{\zeta}|_{\tilde{x}=0}$ denotes the value of $\hat{\zeta}$ on the mid-line λ. The derivative of Eq. (29) with respect to the curvilinear abscissa s leads to:

$$\frac{\partial\hat{\zeta}}{\partial s}=\frac{\partial\hat{\zeta}|_{\tilde{x}=0}}{\partial s}+\left(\varphi_z'-\frac{1}{2}\varphi_x\varphi_y'+\frac{1}{2}\varphi_x'\varphi_y\right)\tilde{x} \tag{30}$$

By substituting Eq. (30) into Eq. (27.b), we obtain:

$$\begin{aligned}\Gamma_{tz}&=2E_{tz}\\&=\left(\xi_c'-\varphi_y+\frac{1}{2}\varphi_x\varphi_z+\varphi_z\eta_c'\right)\frac{dx}{ds}\\&\quad+\left(\eta_c'+\varphi_x+\frac{1}{2}\varphi_y\varphi_z-\varphi_z\xi_c'\right)\frac{dy}{ds}\\&\quad+\left(\varphi_z'-\frac{1}{2}\varphi_x\varphi_y'+\frac{1}{2}\varphi_x'\varphi_y\right)(r+2\tilde{x})+\frac{\partial\hat{\zeta}|_{\tilde{x}=0}}{\partial s}\end{aligned} \tag{31}$$

Despite the usual assumption of zero shear strain along the mid-line λ [1], shear deformations have been modeled according to the theoretical approach proposed by the authors in [7]. In greater detail, the Green strain tensor referred to the local directions $\{\mathbf{n},\mathbf{t},\mathbf{k}\}$ has been represented as follows:

$$\widetilde{\mathbf{E}}=\widetilde{\mathbf{E}}_0+(-\widetilde{\mathbf{E}}_0+\widetilde{\mathbf{E}}_1)+\widetilde{\mathbf{E}}_2=\widetilde{\mathbf{E}}_0+\widetilde{\mathbf{E}}^*+\widetilde{\mathbf{E}}_2. \tag{32}$$

The terms in Eq. (32) have the following meaning ($\overline{E}_{tz}$ indicating the half-angular sliding between the directions $\mathbf{t}$ and $\mathbf{k}$ along the mid-line λ):

$$\widetilde{\mathbf{E}}_1=\begin{bmatrix}0&0&0\\0&0&\overline{E}_{tz}\\0&\overline{E}_{tz}&0\end{bmatrix}\qquad\widetilde{\mathbf{E}}_2=\begin{bmatrix}0&0&0\\0&0&\theta_z\tilde{x}\\0&\theta_z\tilde{x}&E_{zz}\end{bmatrix} \tag{33.a, b}$$

with

$$\theta_z=\varphi_z'-\frac{1}{2}\varphi_x\varphi_y'+\frac{1}{2}\varphi_x'\varphi_y \tag{34}$$

and

$$\widetilde{\mathbf{E}}_0=\mathbf{Q}^{\mathrm{T}}\mathbf{E}_0\mathbf{Q}=\begin{bmatrix}0&0&0\\0&0&\left(E_{xz}^{(0)}\frac{dx}{ds}+E_{yz}^{(0)}\frac{dy}{ds}\right)\\0&\left(E_{xz}^{(0)}\frac{dx}{ds}+E_{yz}^{(0)}\frac{dy}{ds}\right)&0\end{bmatrix} \tag{35}$$

being

$$\mathbf{E}_0=\frac{1}{A}\int_A\mathbf{E}_1\,d\Sigma=\frac{1}{A}\int_A\begin{bmatrix}0&0&\overline{E}_{xz}\\0&0&\overline{E}_{yz}\\\overline{E}_{xz}&\overline{E}_{yz}&0\end{bmatrix}d\Sigma=\begin{bmatrix}0&0&E_{xz}^{(0)}\\0&0&E_{yz}^{(0)}\\E_{xz}^{(0)}&E_{yz}^{(0)}&0\end{bmatrix} \tag{36}$$

$$\mathbf{E}_1=\mathbf{Q}\widetilde{\mathbf{E}}_1\mathbf{Q}^{\mathrm{T}}=\begin{bmatrix}0&0&\overline{E}_{xz}\\0&0&\overline{E}_{yz}\\\overline{E}_{xz}&\overline{E}_{yz}&0\end{bmatrix} \tag{37}$$

The final form of the term $\widetilde{\mathbf{E}}^*$ in Eq. (32) is thereby:

$$\widetilde{\mathbf{E}}^*=(-\widetilde{\mathbf{E}}_0+\widetilde{\mathbf{E}}_1)=\begin{bmatrix}0&0&0\\0&0&E_{tz}^*\\0&E_{tz}^*&0\end{bmatrix} \tag{38}$$

with

$$E_{tz}^*=\overline{E}_{tz}-E_{xz}^{(0)}\frac{dx}{ds}-E_{yz}^{(0)}\frac{dy}{ds} \tag{39}$$

It is worthwhile to note that tensor $\mathbf{E}^*=\mathbf{Q}\widetilde{\mathbf{E}}^*\mathbf{Q}^{\mathrm{T}}$ satisfies the following condition:

$$\int_A\mathbf{E}^*\,d\Sigma=0. \tag{40}$$

Furthermore, it has also been suggested [7] to approximate the term $\Gamma_{tz}^*=2E_{tz}^*$ by separating the dependency on z and s as follows:

$$\Gamma_{tz}^*(s,z)=\Gamma_i(z)f_i(s)\qquad(i=1,2,\ldots,N_s) \tag{41}$$

where f_i are appropriate shape functions and N_s is an integer number. Here the discussion is limited to remarking that these terms provide a more refined modeling of shear deformability along the mid-line λ as the parameter N_s increases. The relevance of shear strains, which are absent in a large number of Vlasov-like theories, is clearly understandable when taking into account the small values of the shear moduli exhibited by pultruded composite beams, which are substantially coincident with those of the resin. The angular sliding thereby assumes the following form:

$$\Gamma_{tz}(s,z)|_{\tilde{x}=0}=\Gamma_x(z)\frac{dx}{ds}+\Gamma_y(z)\frac{dy}{ds}+\Gamma_i(z)f_i(s) \tag{42.a}$$

$$\Gamma_{tz}(\tilde{x},s,z)|_{\tilde{x}\neq0}=\Gamma_{tz}(s,z)|_{\tilde{x}=0}+2\theta_z\tilde{x} \tag{42.b}$$

In Eq. (42) the symbols $\Gamma_x=2E_{xz}^{(0)},\Gamma_y=2E_{yz}^{(0)}$ denote the classical average shear strains while the terms $\Gamma_i(i=1,2,\ldots,N_s)$ act as additional kinematic unknowns.

By comparing Eq. (31), evaluated at $\tilde{x}=0$, with Eq. (42.a), it results:

$$\begin{aligned}\tfrac{\partial\hat{\zeta}|_{\tilde{x}=0}}{\partial s}&=\left(\Gamma_x-\xi_c'+\varphi_y-\tfrac{1}{2}\varphi_x\varphi_z-\varphi_z\eta_c'\right)\tfrac{dx}{ds}\\&\quad+\left(\Gamma_y-\eta_c'-\varphi_x-\frac{1}{2}\varphi_y\varphi_z+\varphi_z\xi_c'\right)\frac{dy}{ds}\\&\quad-\left(\varphi_z'-\frac{1}{2}\varphi_x\varphi_y'+\frac{1}{2}\varphi_x'\varphi_y\right)r+\Gamma_if_i\end{aligned} \tag{43}$$

Furthermore, by integrating Eq. (43) with respect to s, we obtain the final expression of the warping function along the mid-line λ:

$$\hat{\zeta}|_{\tilde{x}=0}=\hat{\zeta}_m-\left(\varphi_z'-\frac{1}{2}\varphi_x\varphi_y'+\frac{1}{2}\varphi_x'\varphi_y\right)\omega(s)+\Gamma_i\omega_i(s) \tag{44}$$

where $\hat{\zeta}_m=\hat{\zeta}|_{\tilde{x}=0,s=0}$ denotes the warping function evaluated at the origin $\mathbf{M}$ of the curvilinear abscissa (Fig. 2), while the terms $\omega(s)$ and $\omega_i(s)$ are defined as follows:

$$\omega(s)=\int_M^{\overline{P}}r(t)dt\qquad\omega_i(s)=\int_M^{\overline{P}}f_i(t)dt \tag{45.a, b}$$

The derivative of Eq. (44) with respect to z, leads to:

$$\frac{\partial\hat{\zeta}|_{\tilde{x}=0}}{\partial z}=\hat{\zeta}_m'-\left(\varphi_z''-\frac{1}{2}\varphi_x\varphi_y''+\frac{1}{2}\varphi_x''\varphi_y\right)\omega(s)+\Gamma_i'\omega_i(s) \tag{46}$$

3.5. Displacement and strain components

For technical applications it is usually possible to discard the dependency of ξ, η and ζ on the local coordinate $\tilde{x}$ (i.e. small thickness), thus giving to the displacement field the following final form:

$$\begin{aligned}\xi\cong\xi|_{\tilde{x}=0}&=\xi_c-\frac{1}{2}\left(\varphi_y^2+\varphi_z^2\right)(x-x_c)\\&\quad+\left(-\varphi_z+\frac{1}{2}\varphi_x\varphi_y\right)(y-y_c)\end{aligned} \tag{47.a}$$

$$\begin{aligned}\eta\cong\eta|_{\tilde{x}=0}&=\eta_c+\left(\varphi_z+\frac{1}{2}\varphi_x\varphi_y\right)(x-x_c)\\&\quad-\frac{1}{2}(\varphi_x^2+\varphi_z^2)(y-y_c)\end{aligned} \tag{47.b}$$

Please cite this article in press as: Mancusi G, Feo L. Non-linear pre-buckling behavior of shear deformable thin-walled composite beams with open cross-section. Composites: Part B (2012), http://dx.doi.org/10.1016/j.compositesb.2012.11.003

$$\zeta \cong \zeta|_{\tilde{x}=0} = \zeta_m + \left(-\varphi_y + \frac{1}{2}\varphi_x\varphi_z\right)(x - x_m) + \left(\varphi_x + \frac{1}{2}\varphi_y\varphi_z\right)(y - y_m) - \left(\varphi'_z - \frac{1}{2}\varphi_x\varphi'_y + \frac{1}{2}\varphi'_x\varphi_y\right)\omega(s) + \Gamma_i\omega_i(s) \quad (47.c)$$

where $\zeta_m = \zeta|_{\tilde{x}=0,s=0}$ denotes the axial displacement evaluated at the origin **M** of the curvilinear abscissa (Fig. 2). Finally, from Eq. (42.b), it is:

$$\Gamma_{tz} = \Gamma_x(z)\frac{dx}{ds} + \Gamma_y(z)\frac{dy}{ds} + \Gamma_i(z)f_i(s) + 2\left(\varphi'_z - \frac{1}{2}\varphi_x\varphi'_y + \frac{1}{2}\varphi'_x\varphi_y\right)\tilde{x} \quad (48.a)$$

while from Eq. (24.c) and Eq. (46) it descends:

$$E_{33} \cong E_{33}|_{\tilde{x}=0} = \zeta'_m - \left(\varphi'_y - \frac{1}{2}\varphi_x\varphi'_z - \frac{1}{2}\varphi'_x\varphi_z\right)(x - x_m) + \left(\varphi'_x + \frac{1}{2}\varphi_y\varphi'_z + \frac{1}{2}\varphi'_y\varphi_z\right)(y - y_m) + \varphi'_z\eta'_c(x - x_c) - \varphi'_z\xi'_c(y - y_c) - \left(\varphi''_z - \frac{1}{2}\varphi_x\varphi''_y + \frac{1}{2}\varphi''_x\varphi_y\right)\omega + \Gamma'_i\omega_i + \frac{1}{2}(\xi'_c)^2 + \frac{1}{2}(\eta'_c)^2 + \frac{1}{2}\left[\left(\varphi'_y\right)^2 + (\varphi'_z)^2\right](x - x_c)^2 + \frac{1}{2}\left[(\varphi'_x)^2 + (\varphi'_z)^2\right](y - y_c)^2 - \varphi'_x\varphi'_y(x - x_c)(y - y_c) \quad (48.b)$$

It is useful to rewrite Eq. (48) as follows:

$$\Gamma_{tz} = \Gamma_x\frac{dx}{ds} + \Gamma_y\frac{dy}{ds} + \Gamma_i f_i + 2\theta_z\tilde{x} \quad (49.a)$$

$$E_{33} \cong a + \theta_x y - \theta_y x + \theta_0\omega + \psi_{xx}y^2 + \psi_{yy}x^2 + \psi_{xy}xy + \psi_{zz}(x^2 + y^2) + \Gamma'_i\omega_i \quad (49.b)$$

The following generalized strains can be, in fact, identified in addition to Γ_x, Γ_y, Γ_i/Γ'_i and θ_z:

$$a = \zeta'_m + \left(\varphi'_y - \frac{1}{2}\varphi_x\varphi'_z - \frac{1}{2}\varphi'_x\varphi_z\right)x_m - \left(\varphi'_x + \frac{1}{2}\varphi_y\varphi'_z + \frac{1}{2}\varphi'_y\varphi_z\right)y_m - \varphi'_z\eta'_c x_c + \varphi'_z\xi'_c y_c + \frac{1}{2}(\xi'_c)^2 + \frac{1}{2}(\eta'_c)^2 + \frac{1}{2}\left[\left(\varphi'_y\right)^2 + (\varphi'_z)^2\right]x_c^2 + \frac{1}{2}\left[(\varphi'_x)^2 + (\varphi'_z)^2\right]y_c^2 - \varphi'_x\varphi'_y x_c y_c \quad (50.a)$$

$$\theta_x = \varphi'_x + \frac{1}{2}\varphi_y\varphi'_z + \frac{1}{2}\varphi'_y\varphi_z - \varphi'_z\xi'_c - \left[(\varphi'_x)^2 + (\varphi'_z)^2\right]y_c + \varphi'_x\varphi'_y x_c \quad (50.b)$$

$$\theta_y = \varphi'_y - \frac{1}{2}\varphi_x\varphi'_z - \frac{1}{2}\varphi'_x\varphi_z - \varphi'_z\eta'_c + \left[\left(\varphi'_y\right)^2 + (\varphi'_z)^2\right]x_c - \varphi'_x\varphi'_y y_c \quad (50.c)$$

$$\theta_0 = -\varphi''_z + \frac{1}{2}\varphi_x\varphi''_y - \frac{1}{2}\varphi''_x\varphi_y \quad (50.d)$$

$$\psi_{xx} = \frac{1}{2}(\varphi'_x)^2 \quad (50.e)$$

$$\psi_{yy} = \frac{1}{2}\left(\varphi'_y\right)^2 \quad (50.f)$$

$$\psi_{xy} = -\varphi'_x\varphi'_y \quad (50.g)$$

$$\psi_{zz} = \frac{1}{2}(\varphi'_z)^2 \quad (50.h)$$

3.6. Stress tensor

The second Piola–Kirchhoff symmetric stress tensor can be expressed in the following form:

$$\tilde{\mathbf{S}} = \begin{bmatrix} S_{nn} & S_{nt} & S_{nz} \\ S_{nt} & S_{tt} & S_{tz} \\ S_{nz} & S_{tz} & S_{zz} \end{bmatrix} \quad (51)$$

Due to the assumptions introduced above, it results that S_{tz} and S_{zz} are conjugated with the non-trivial strains E_{tz} and E_{zz}, respectively.

A general form of the stress–strain relationship has been previously provided [27], which accounts for an arbitrary orientation of the fibers, allowing to analyze the behavior of a generic laminated beam. Examples relative to the application of a reduced linear form of the present model, which accounts for a generic orientation of the fibers, are given in [28,29].

As indicated in Section 4, however, in view of investigating the behavior of pultruded beams (which are more sensitive to shear deformations), a simplified stress–strain relationship can be assumed.

The appropriate choice of the stress–strain relationship should also account for possible influence of creep strains over time. Creep strains, which can be very relevant [30–32], can be seen, in fact, as an evolving geometric not-negligible defect, which provokes a time evolution of the non-linear response of the composite beam. The mechanical model, however, in its version here presented does not account yet for this.

3.7. Variational formulation

In view of a variational formulation of the equilibrium for the beam under consideration, the virtual work done by the internal stresses can be proposed in the following form:

$$\delta L_i = \int_0^L \left(T_x\delta\Gamma_x + T_y\delta\Gamma_y + \Lambda_i\delta\Gamma_i + M_z\delta\theta_z + N\delta a + M_x\delta\theta_x + M_y\delta\theta_y + W_0\delta\theta_0 + P_{xx}\delta\psi_{xx} + P_{yy}\delta\psi_{yy} + P_{xy}\delta\psi_{xy} + P_{zz}\delta\psi_{zz} + W_i\delta\Gamma'_i\right)dz \quad (52)$$

where δ indicates the variational operator.

In Eq. (52) the following positions have been considered:

$$T_x = \int_A S_{tz}\frac{dx}{ds}d\Sigma \quad T_y = \int_A S_{tz}\frac{dy}{ds}d\Sigma \quad (53.a, b)$$

$$\Lambda_i = \int_A S_{tz}f_i d\Sigma \quad M_z = 2\int_A S_{tz}\tilde{x}d\Sigma \quad (53.c, d)$$

and

$$N = \int_A S_{zz}d\Sigma \quad M_x = \int_A S_{zz}y d\Sigma \quad M_y = -\int_A S_{zz}x d\Sigma \quad (54.a\text{-}c)$$

$$W_0 = \int_A S_{zz}\omega d\Sigma \quad P_{xx} = \int_A S_{zz}y^2 d\Sigma \quad P_{yy} = \int_A S_{zz}x^2 d\Sigma \quad (54.d\text{-}f)$$

$$P_{xy} = \int_A S_{zz}xy d\Sigma \quad P_{zz} = \int_A S_{zz}(x^2 + y^2)d\Sigma \quad (54.g, h)$$

$$W_i = \int_A S_{zz}\omega_i d\Sigma \quad (54.i)$$

On the other hand, the virtual work done by the external loads can be represented as:

$$\delta L_e = \int_0^L dz\int_A (\mathbf{b}\delta\mathbf{u})d\Sigma + \int_0^L dz\int_{\partial A}(\mathbf{p}\delta\mathbf{u})d\Sigma + \int_{\Sigma_{(\alpha)}}(\mathbf{p}\delta\mathbf{u})d\Sigma \quad (55)$$

where

- $\mathbf{b} = [b_x, b_y, b_z]^T$ is the external force for unit volume;
- $\mathbf{p} = [p_x, p_y, p_z]^T$ is the external force for unit surface acting on the boundary of the beam;
- $\mathbf{u} = [\xi, \eta, \zeta]^T$ is the displacement field vector given by Eq. (47);
- $\alpha = 1,2$ is a parameter indicating the ends of the beam ($\Sigma_{(1)}$ or $\Sigma_{(2)}$).

It results:

Please cite this article in press as: Mancusi G, Feo L. Non-linear pre-buckling behavior of shear deformable thin-walled composite beams with open cross-section. Composites: Part B (2012), http://dx.doi.org/10.1016/j.compositesb.2012.11.003

$$\begin{aligned}\delta L_e = \int_0^L \Big[& q_x\delta\xi_c + q_y\delta\eta_c + q_z\delta\zeta_m - w_0\delta\varphi_z' + w_i\delta\Gamma_i - \frac{1}{2}w_0\varphi_y\delta\varphi_x' \\ & + \frac{1}{2}w_0\varphi_x\delta\varphi_y' + \left(m_x - \frac{1}{2}m_y\varphi_z + \frac{1}{2}w_0\varphi_y' + \frac{1}{2}n_z\varphi_y - n_y\varphi_x\right)\delta\varphi_x \\ & + \left(m_y + \frac{1}{2}m_x\varphi_z - \frac{1}{2}w_0\varphi_x' + \frac{1}{2}n_z\varphi_x - n_x\varphi_y\right)\delta\varphi_y \\ & + \left(m_z + \frac{1}{2}m_x\varphi_y - \frac{1}{2}m_y\varphi_x - (n_x+n_y)\varphi_z\right)\delta\varphi_z\Big]\mathrm{d}z Q_x^{(\alpha)}\delta\xi_c^{(\alpha)} \\ & + Q_y^{(\alpha)}\delta\eta_c^{(\alpha)} + Q_z^{(\alpha)}\delta\zeta_m^{(\alpha)} - W_0^{(\alpha)}\delta\varphi_z'^{(\alpha)} + W_i^{(\alpha)}\delta\Gamma_i^{(\alpha)} \\ & - \frac{1}{2}W_0^{(\alpha)}\varphi_y^{(\alpha)}\delta\varphi_x'^{(\alpha)} + \frac{1}{2}W_0^{(\alpha)}\varphi_x^{(\alpha)}\delta\varphi_y'^{(\alpha)} \\ & + \left(C_x^{(\alpha)} - \frac{1}{2}C_y^{(\alpha)}\varphi_z^{(\alpha)} + \frac{1}{2}W_0^{(\alpha)}\varphi_y'^{(\alpha)} + \frac{1}{2}N_z^{(\alpha)}\varphi_y^{(\alpha)} - N_y^{(\alpha)}\varphi_x^{(\alpha)}\right)\delta\varphi_x^{(\alpha)} \\ & + \left(C_y^{(\alpha)} + \frac{1}{2}C_x^{(\alpha)}\varphi_z^{(\alpha)} - \frac{1}{2}W_0^{(\alpha)}\varphi_x'^{(\alpha)} + \frac{1}{2}N_z^{(\alpha)}\varphi_x^{(\alpha)} - N_x^{(\alpha)}\varphi_y^{(\alpha)}\right)\delta\varphi_y^{(\alpha)} \\ & + \left(C_z^{(\alpha)} + \frac{1}{2}C_x^{(\alpha)}\varphi_y^{(\alpha)} - \frac{1}{2}C_y^{(\alpha)}\varphi_x^{(\alpha)} - \left(N_x^{(\alpha)} + N_y^{(\alpha)}\right)\varphi_z^{(\alpha)}\right)\delta\varphi_z^{(\alpha)}\end{aligned} \tag{56}$$

where

$$q_x = \int_A b_x\mathrm{d}\Sigma + \int_{\partial A} p_x\mathrm{d}s \quad q_y = \int_A b_y\mathrm{d}\Sigma + \int_{\partial A} p_y\mathrm{d}s \tag{57.a, b}$$

$$q_z = \int_A b_z\mathrm{d}\Sigma + \int_{\partial A} p_z\mathrm{d}s \tag{57.c}$$

$$m_x = \int_A b_z(y-y_m)\mathrm{d}\Sigma + \int_{\partial A} p_z(y-y_m)\mathrm{d}s \tag{57.d}$$

$$m_y = -\int_A b_z(x-x_m)\mathrm{d}\Sigma - \int_{\partial A} p_z(x-x_m)\mathrm{d}s \tag{57.e}$$

$$\begin{aligned} m_z = & \int_A [-b_x(y-y_c) + b_y(x-x_c)]\mathrm{d}\Sigma \\ & + \int_{\partial A} [-p_x(y-y_c) + p_y(x-x_c)]\mathrm{d}s \end{aligned} \tag{57.f}$$

$$w_0 = \int_A b_z\omega\mathrm{d}\Sigma + \int_{\partial A} p_z\omega\mathrm{d}s \tag{57.g}$$

$$w_i = \int_A b_z\omega_i\mathrm{d}\Sigma + \int_{\partial A} p_z\omega_i\mathrm{d}s \tag{57.h}$$

$$n_x = \int_A b_x(x-x_c)\mathrm{d}\Sigma + \int_{\partial A} p_x(x-x_c)\mathrm{d}s \tag{57.i}$$

$$n_y = \int_A b_y(y-y_c)\mathrm{d}\Sigma + \int_{\partial A} p_y(y-y_c)\mathrm{d}s \tag{57.j}$$

$$\begin{aligned} n_z = & \int_A [b_x(y-y_c) + b_y(x-x_c)]\mathrm{d}\Sigma \\ & + \int_{\partial A} [p_x(y-y_c) + p_y(x-x_c)]\mathrm{d}s \end{aligned} \tag{57.k}$$

and

$$Q_x^{(\alpha)} = \int_{\Sigma_{(\alpha)}} p_x\mathrm{d}\Sigma \quad Q_y^{(\alpha)} = \int_{\Sigma_{(\alpha)}} p_y\mathrm{d}\Sigma \quad Q_z^{(\alpha)} = \int_{\Sigma_{(\alpha)}} p_z\mathrm{d}\Sigma \tag{58.a-c}$$

$$C_x^{(\alpha)} = \int_{\Sigma_{(\alpha)}} p_z(y-y_m)\mathrm{d}\Sigma \quad C_y^{(\alpha)} = -\int_{\Sigma_{(\alpha)}} p_z(x-x_m)\mathrm{d}\Sigma \tag{58.d, e}$$

$$C_z^{(\alpha)} = \int_{\Sigma_{(\alpha)}} [-p_x(y-y_c) + p_y(x-x_c)]\mathrm{d}\Sigma \tag{58.f}$$

$$W_0^{(\alpha)} = \int_{\Sigma_{(\alpha)}} p_z\omega\mathrm{d}\Sigma \qquad W_i^{(\alpha)} = \int_{\Sigma_{(\alpha)}} p_z\omega_i\mathrm{d}\Sigma \tag{58.g, h}$$

$$N_x^{(\alpha)} = \int_{\Sigma_{(\alpha)}} p_x(x-x_c)\mathrm{d}\Sigma \quad N_y^{(\alpha)} = \int_{\Sigma_{(\alpha)}} p_y(x-x_c)\mathrm{d}\Sigma \tag{58.i, j}$$

$$N_z^{(\alpha)} = \int_{\Sigma_{(\alpha)}} [p_x(y-y_c) + p_y(x-x_c)]\mathrm{d}\Sigma \tag{58.k}$$

Finally, the principle of virtual displacements implies:

$$\int_0^L \mathbf{s}\cdot\delta\mathbf{e}\mathrm{d}z = \int_0^L (\mathbf{q} + \mathbf{H}\mathbf{v})\delta\mathbf{v}\mathrm{d}z + (\mathbf{Q}^{(\alpha)} + \mathbf{H}^{(\alpha)}\mathbf{v}^{(\alpha)})\delta\mathbf{v}^{(\alpha)} \tag{59}$$

where

$$\mathbf{s} = [T_x, T_y, \Lambda_1, \cdots, \Lambda_i, \cdots, \Lambda_{N_s}, M_z, N, M_x, M_y, W_0, P_{xx}, P_{yy}, P_{xy}, P_{zz}, W_1, \cdots, W_i, \cdots, W_{N_s}]^{\mathrm{T}} \tag{60.a}$$

$$\mathbf{e} = [\Gamma_x, \Gamma_y, \Gamma_1, \cdots, \Gamma_i, \cdots, \Gamma_{N_s}, \theta_z, a, \theta_x, \theta_y, \theta_0, \psi_{xx}, \psi_{yy}, \psi_{xy}, \psi_{zz}, \Gamma_1', \cdots, \Gamma_i', \cdots, \Gamma_{N_s}']^{\mathrm{T}} \tag{60.b}$$

$$\mathbf{q} = [q_x, q_y, q_z, m_x, 0, m_y, 0, m_z, -w_0, w_1, \cdots, w_i, \cdots, w_{N_s}]^{\mathrm{T}} \tag{60.c}$$

$$\mathbf{H} = \begin{bmatrix}
0&0&0&0&0&0&0&0&0&0&\cdots&0&\cdots&0\\
0&0&0&0&0&0&0&0&0&0&\cdots&0&\cdots&0\\
0&0&0&0&0&0&0&0&0&0&\cdots&0&\cdots&0\\
0&0&0&-n_y&0&\frac{1}{2}n_z&\frac{1}{2}w_0&-\frac{1}{2}m_y&0&0&\cdots&0&\cdots&0\\
0&0&0&0&0&-\frac{1}{2}w_0&0&0&0&0&\cdots&0&\cdots&0\\
0&0&0&\frac{1}{2}n_z&-\frac{1}{2}w_0&-n_x&0&\frac{1}{2}m_x&0&0&\cdots&0&\cdots&0\\
0&0&0&\frac{1}{2}w_0&0&0&0&0&0&0&\cdots&0&\cdots&0\\
0&0&0&-\frac{1}{2}m_y&0&\frac{1}{2}m_x&0&-(n_x+n_y)&0&0&\cdots&0&\cdots&0\\
0&0&0&0&0&0&0&0&0&0&\cdots&0&\cdots&0\\
0&0&0&0&0&0&0&0&0&0&\cdots&0&\cdots&0\\
\vdots&\vdots&\vdots&\vdots&\vdots&\vdots&\vdots&\vdots&\vdots&\vdots&\ddots&&&\vdots\\
0&0&0&0&0&0&0&0&0&0&&0&&0\\
\vdots&\vdots&\vdots&\vdots&\vdots&\vdots&\vdots&\vdots&\vdots&\vdots&&&\ddots&\vdots\\
0&0&0&0&0&0&0&0&0&0&\cdots&0&\cdots&0
\end{bmatrix} \tag{60.d}$$

$$\mathbf{v} = \left[\xi_c, \eta_c, \zeta_m, \varphi_x, \varphi_x', \varphi_y, \varphi_y', \varphi_z, \varphi_z', \Gamma_1, \cdots, \Gamma_i, \cdots, \Gamma_{N_s}\right]^{\mathrm{T}} \tag{60.e}$$

$$\mathbf{Q}^{(\alpha)} = \left[Q_x^{(\alpha)}, Q_y^{(\alpha)}, Q_z^{(\alpha)}, C_x^{(\alpha)}, 0, C_y^{(\alpha)}, 0, C_z^{(\alpha)}, -W_0^{(\alpha)}, W_1^{(\alpha)}, \cdots, W_i^{(\alpha)}, \cdots, W_{N_s}^{(\alpha)}\right]^{\mathrm{T}} \tag{60.f}$$

$$\mathbf{H}^{(\alpha)} = \begin{bmatrix}
0&0&0&0&0&0&0&0&0&0&\cdots&0&\cdots&0\\
0&0&0&0&0&0&0&0&0&0&\cdots&0&\cdots&0\\
0&0&0&0&0&0&0&0&0&0&\cdots&0&\cdots&0\\
0&0&0&-N_y^{(\alpha)}&0&\frac{1}{2}N_z^{(\alpha)}&\frac{1}{2}W_0^{(\alpha)}&-\frac{1}{2}C_y^{(\alpha)}&0&0&\cdots&0&\cdots&0\\
0&0&0&0&0&-\frac{1}{2}W_0^{(\alpha)}&0&0&0&0&\cdots&0&\cdots&0\\
0&0&0&\frac{1}{2}N_z^{(\alpha)}&-\frac{1}{2}W_0^{(\alpha)}&-N_x^{(\alpha)}&0&\frac{1}{2}C_x^{(\alpha)}&0&0&\cdots&0&\cdots&0\\
0&0&0&\frac{1}{2}W_0^{(\alpha)}&0&0&0&0&0&0&\cdots&0&\cdots&0\\
0&0&0&-\frac{1}{2}C_y^{(\alpha)}&0&\frac{1}{2}C_x^{(\alpha)}&0&-(N_x^{(\alpha)}+N_y^{(\alpha)})&0&0&\cdots&0&\cdots&0\\
0&0&0&0&0&0&0&0&0&0&\cdots&0&\cdots&0\\
0&0&0&0&0&0&0&0&0&0&\cdots&0&\cdots&0\\
\vdots&\vdots&\vdots&\vdots&\vdots&\vdots&\vdots&\vdots&\vdots&\vdots&\ddots&&&\vdots\\
0&0&0&0&0&0&0&0&0&0&&0&&0\\
\vdots&\vdots&\vdots&\vdots&\vdots&\vdots&\vdots&\vdots&\vdots&\vdots&&&\ddots&\vdots\\
0&0&0&0&0&0&0&0&0&0&\cdots&0&\cdots&0
\end{bmatrix} \tag{60.g}$$

$$\mathbf{v}^{(\alpha)} = \left[\xi_c^{(\alpha)}, \eta_c^{(\alpha)}, \zeta_m^{(\alpha)}, \varphi_x^{(\alpha)}, \varphi_x'^{(\alpha)}, \varphi_y^{(\alpha)}, \varphi_y'^{(\alpha)}, \varphi_z^{(\alpha)}, \varphi_z'^{(\alpha)}, \Gamma_1^{(\alpha)}, \cdots, \Gamma_i^{(\alpha)}, \cdots, \Gamma_{N_s}^{(\alpha)}\right]^{\mathrm{T}} \tag{60.h}$$

Please cite this article in press as: Mancusi G, Feo L. Non-linear pre-buckling behavior of shear deformable thin-walled composite beams with open cross-section. Composites: Part B (2012), http://dx.doi.org/10.1016/j.compositesb.2012.11.003

3.8. Cross-section made of interconnected thin rectangles

When dealing with common structural shapes, the open cross-sections can be seen as made of interconnected thin-rectangles. As a consequence, the mid-line λ can be represented as follows:

$$\lambda = \bigcup_{p=1,N_{seg}} \lambda_p \tag{61}$$

where λ_p denotes the intersection between λ and the generic pth rectangle, while N_{seg} indicates the overall number of rectangles.

As already indicated, it has been suggested to separate the dependency of Γ^*_{tz} on the curvilinear abscissa s from the one on the axial coordinate z, according to the general form given in Eq. (41).

With this aim the following positions can be introduced:

$$h_p^{(q)}(s) = \begin{cases} (q+1)(s-s_p)^q & s \in \lambda_p \quad (p = 1,2,\ldots,N_{seg}) \\ 0 & elsewhere \quad (q = 0,1,\ldots,N_o) \end{cases} \tag{62}$$

where s_p is the curvilinear abscissa evaluated at the first end of the pth rectangle and N_o ($N_o \geqslant 1$) is a fixed integer denoting the maximum order of the polynomial approximation of Γ^*_{tz}.

By means of Eq. (62), it is possible to rewrite Eq. (41) as follows:

$$\Gamma^*_{tz}(s,z) = \Gamma_p^{(q)}(z) h_p^{(q)}(s) \quad \begin{matrix} (p = 1,2,\ldots,N_{seg}) \\ (q = 0,1,\ldots,N_o) \end{matrix} \tag{63}$$

Furthermore, the following linear equations must be introduced in order to satisfy Eq. (40):

$$\Gamma_p^{(q)} \omega_{p,q}^{(xz)} = 0 \quad \Gamma_p^{(q)} \omega_{p,q}^{(yz)} = 0 \tag{64.a, b}$$

where

$$\omega_{p,q}^{(xz)} = \int_\lambda h_p^{(q)}(s) \frac{dx}{ds} b\, ds \quad \omega_{p,q}^{(yz)} = \int_\lambda h_p^{(q)}(s) \frac{dy}{ds} b\, ds \tag{65.a, b}$$

It is generally possible to find four integer numbers:

$$p_1, p_2 \in \{1,2,\ldots,N_{seg}\} \quad q_1, q_2 \in \{0,1,\ldots,N_o\} \tag{66.a, b}$$

ensuring that

$$\Delta = \omega_{p_1,q_1}^{(xz)} \omega_{p_2,q_2}^{(yz)} - \omega_{p_2,q_2}^{(xz)} \omega_{p_1,q_1}^{(yz)} \neq 0 \tag{67}$$

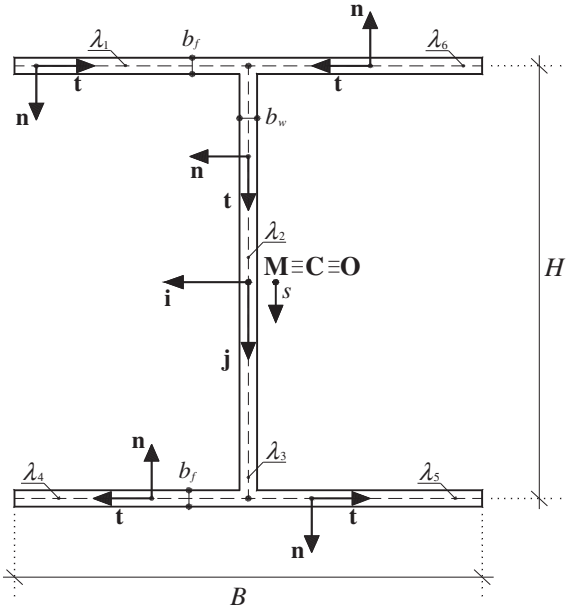

Fig. 3. I-section (N_{seg} = 6).

If Eq. (67) is satisfied, then the two unknowns $\Gamma_{p_1}^{(q_1)}(z)$ and $\Gamma_{p_2}^{(q_2)}(z)$ can be expressed via the following two linear combinations:

$$\Gamma_{p_1}^{(q_1)} = a_{mn} \Gamma_m^{(n)} \quad \Gamma_{p_2}^{(q_2)} = b_{mn} \Gamma_m^{(n)} \tag{68.a, b}$$

where

$$(m,n) \in \{1,2,\ldots,N_{seg}\} \times \{0,1,\ldots,N_o\} - \{(p_1,q_1),(p_2,q_2)\} \tag{69}$$

Finally, Γ^*_{tz} can be expressed in the following form:

$$\begin{aligned} \Gamma^*_{tz}(s,z) &= \Gamma_p^{(q)}(z) h_p^{(q)}(s) \\ &= \Gamma_{p_1}^{(q_1)}(z) h_{p_1}^{(q_1)}(s) + \Gamma_{p_2}^{(q_2)}(z) h_{p_2}^{(q_2)}(s) + \Gamma_m^{(n)}(z) h_m^{(n)}(s) \\ &= \Gamma_m^{(n)} (a_{mn} h_{p_1}^{(q_1)} + b_{mn} h_{p_2}^{(q_2)} + h_m^{(n)}) = \Gamma_m^{(n)} f_m^{(n)} \end{aligned} \tag{70}$$

It should be noted that the required shape functions f_i with $i \in \{1,2,\ldots,N_s\}$ and $N_s = N_{seg} \times (N_o + 1) - 2$), correspond to simply renumbering of the functions $f_m^{(n)}$, generated as above.

An example concerning a symmetric I-section is presented in Fig. 3.

The functions $h_p^{(q)}$ obtained for the generic symmetric I-section in Fig. 3 are presented in Table 1. As expected, the p index varies within the set {1,2,…,6} while the q index, which denotes the exponent of the current polynomial, is still indeterminate. If, for examples, it is assumed N_o = 2, then N_s is equal to 16. It is important to remark that within this theory the accuracy of predicted shear deformations depends on the maximum order N_o of polynomials $h_p^{(q)}$.

It easy to verify that the following choice:

$$p_1 = 1 \quad p_2 = 2 \quad q_1 = 0 \quad q_2 = 0 \tag{71.a-d}$$

leads to

$$\Delta = \omega_{1,0}^{(xz)} \omega_{2,0}^{(yz)} - \omega_{2,0}^{(xz)} \omega_{1,0}^{(yz)} = -\frac{1}{4} b_f b_w BH \neq 0 \tag{72}$$

thus ensuring the possibility to express $\Gamma_1^{(0)}$ and $\Gamma_2^{(0)}$ by virtue of Eq. (68.a,b).

Finally, the resulting functions for N_o = 2(i = 1,2,…,16) are presented in Table 2.

3.9. Finite element approximation

The variational equilibrium equation Eq. (59) has been formulated via a numerical model based on a finite element approximation. The mesh proposed is composed of finite elements characterized by $2 \times (12 + 2N_s)$ degrees of freedom, including $(12 + 2N_s)$ d.o.f. per each node i (i = 1,2). (see Table 3).

Let u be the generic kinematic un-known. The approximation of u is obtained by cubic interpolating polynomials as follows:

$$u(\xi) = \mathrm{h}_{10}(\xi) u_1 + \mathrm{h}_{11}(\xi) u_1' + \mathrm{h}_{20}(\xi) u_2 + \mathrm{h}_{21}(\xi) u_2' \tag{73}$$

where

$$\mathrm{h}_{10} = \frac{1}{4}(2 - 3\xi + \xi^3) \quad \mathrm{h}_{11} = \frac{l_e}{8}(1 - \xi - \xi^2 + \xi^3) \tag{74.a, b}$$

$$\mathrm{h}_{20} = \frac{1}{4}(2 + 3\xi - \xi^3) \quad \mathrm{h}_{21} = \frac{l_e}{8}(-1 - \xi + \xi^2 + \xi^3) \tag{74.c, d}$$

being l_e the length of the finite element; u_1 and u_2 the nodal values of the kinematic un-known under consideration while u_1' and u_2' the nodal values of the derivative of u with respect to the axial coordinate z (see Fig. 4).

4. Numerical comparisons

The kinematic model discussed in previous Section 3 has been applied to the study of a composite pultruded cantilever beam

Table 1
Functions $h_p^{(q)}$ for the generic symmetric I-section shown in Fig. 3 ($q = 0,1,\ldots,N_o$).

	$s \in \lambda_1$	$s \in \lambda_2$	$s \in \lambda_3$	$s \in \lambda_4$	$s \in \lambda_5$	$s \in \lambda_6$
$h_1^{(q)}$	$(q+1)(s+\frac{B}{2}+\frac{H}{2})^q$	0	0	0	0	0
$h_2^{(q)}$	0	$(q+1)(s+\frac{H}{2})^q$	0	0	0	0
$h_3^{(q)}$	0	0	$(q+1)s^q$	0	0	0
$h_4^{(q)}$	0	0	0	$(q+1)(s-\frac{H}{2})^q$	0	0
$h_5^{(q)}$	0	0	0	0	$(q+1)(s-\frac{H}{2})^q$	0
$h_6^{(q)}$	0	0	0	0	0	$(q+1)(s+\frac{B}{2}+\frac{H}{2})^q$

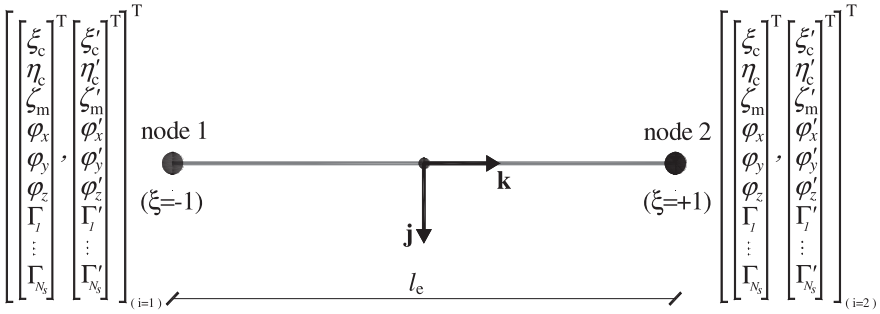

Fig. 4. Finite element.

Table 2
Functions f_i for the generic symmetric I-section shown in Fig. 3 ($N_o = 2$).

f_i	m	n	$f_m^{(n)}$	f_i	m	n	$f_m^{(n)}$
f_1	1	1	$h_1^{(1)} - \frac{B}{2}h_1^{(0)}$	f_9	4	1	$h_4^{(1)} + \frac{B}{2}h_1^{(0)}$
f_2	1	2	$h_1^{(2)} - \frac{B^2}{4}h_1^{(0)}$	f_{10}	4	2	$h_4^{(2)} + \frac{B^2}{4}h_1^{(0)}$
f_3	2	1	$h_2^{(1)} - \frac{H}{2}h_2^{(0)}$	f_{11}	5	0	$h_5^{(0)} - h_1^{(0)}$
f_4	2	2	$h_2^{(2)} - \frac{H^2}{4}h_2^{(0)}$	f_{12}	5	1	$h_5^{(1)} - \frac{B}{2}h_1^{(0)}$
f_5	3	0	$h_3^{(0)} - h_2^{(0)}$	f_{13}	5	2	$h_5^{(2)} - \frac{B^2}{4}h_1^{(0)}$
f_6	3	1	$h_3^{(1)} - \frac{H}{2}h_2^{(0)}$	f_{14}	6	0	$h_6^{(0)} + h_1^{(0)}$
f_7	3	2	$h_3^{(2)} - \frac{H^2}{4}h_2^{(0)}$	f_{15}	6	1	$h_6^{(1)} + \frac{B}{2}h_1^{(0)}$
f_8	4	0	$h_4^{(0)} + h_1^{(0)}$	f_{16}	6	2	$h_6^{(2)} + \frac{B^2}{4}h_1^{(0)}$

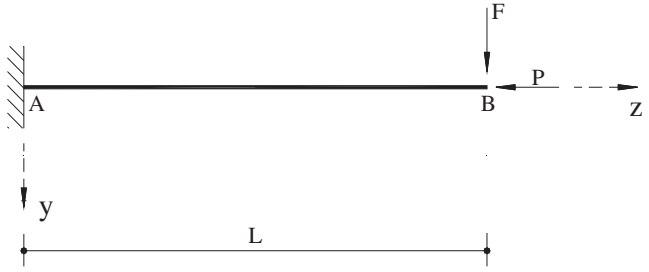

Fig. 5. Examined cantilever beam.

Table 3
Degrees of freedom.

	"a"	"b"	"c"
N_s	0	0	16
Nodal d.o.f.	12	12	44
Overall d.o.f.	1212	1212	4444

Table 4
Load multiplier λ_F versus normalized axial force v.

v	$\alpha = 1$			$\alpha = 5$		
	"a"	"b"	"c"	"a"	"b"	"c"
0.3	15.56	14.67	13.14	8.88	8.77	8.57
0.6	15.22	14.36	12.96	8.16	8.05	7.99

made of Carbon Fiber-Reinforced Polymer (CFRP) under the combined action of a fixed compressive axial force P and an increasing transverse force F acting at the centroid of the free end (Fig. 5).

The cross section shown in Fig. 3 has been considered, with the geometric parameters assuming the following values: $B = 50$ mm, $H = 47$ mm, $b_f = b_w = 3$ mm. It is worth noting that the cross-section is the same considered in [27].

In relation to the constitutive behavior of the composite, a linear elastic stress–strain relationship has been assumed according to the following simplified law:

$$\begin{bmatrix} S_{tz} \\ S_{zz} \end{bmatrix} = \begin{bmatrix} G_{tz} & 0 \\ 0 & D_{zz} \end{bmatrix} \begin{bmatrix} \Gamma_{tz} \\ E_{zz} \end{bmatrix} \tag{75}$$

being D_{zz} the longitudinal normal modulus while G_{tz} the shear modulus relative to the directions **t** and **k**. Due to the considered orientation of the fibers, which are aligned to the **k** unit vector, the out of diagonal terms are not present. Moreover, it has been assumed $D_{zz} = 138000$ N/mm^2 and $G_{tz} = 5170$ N/mm^2, which correspond to the material denoted by "M2" in [27].

The flexural, torsional and warping rigidity constants of the cross-section are:

$$D_{zz}I_{xx} = 2.648 \times 10^{10}\ \text{N mm}^2 \tag{76.a}$$

$$D_{zz}I_{yy} = 8.640 \times 10^{9}\ \text{N mm}^2 \tag{76.b}$$

$$G_{tz}J_t = 6.840 \times 10^{6}\ \text{N mm}^2 \tag{76.c}$$

$$D_{zz}\Pi_\omega = 4.763 \times 10^{12}\ \text{N mm}^4 \tag{76.d}$$

Please cite this article in press as: Mancusi G, Feo L. Non-linear pre-buckling behavior of shear deformable thin-walled composite beams with open cross-section. Composites: Part B (2012), http://dx.doi.org/10.1016/j.compositesb.2012.11.003

Table 5a
dimensionless deflection δ at $z = L$ ($\alpha = 1$).

v	λ_F	Linear analysis			Non-linear analysis		
		"a"	"b"	"c"	"a"	"b"	"c"
0.3	13.14	1.000	1.158	1.178	1.107	1.297	1.322
0.6	12.96	1.000	1.158	1.178	1.240	1.475	1.507

Table 5b
dimensionless flexural rotation γ at $z = L$ ($\alpha = 1$).

v	λ_F	Linear analysis			Non-linear analysis		
		"a"	"b"	"c"	"a"	"b"	"c"
0.3	13.14	1.000	1.001	1.015	1.111	1.128	1.147
0.6	12.96	1.000	1.001	1.015	1.250	1.292	1.317

Furthermore, the following slenderness parameter is introduced:

$$\alpha = \frac{G_{tz} J_t L^2}{D_{zz} \Pi_\omega} \tag{77}$$

which, within the analyses carried out, has been assumed equal to $\alpha = 1$ or $\alpha = 5$.

The results have been presented with the aim of analyzing the critical values of the external loads and the coupling effect between deformability in shear and geometric non-linearity.

Despite of the model proposed in [27], the present analysis accounts, in fact, for the shear deformability of the mid-surface of the thin-walled beam by means at least of the average shear strains Γ_x and Γ_y; if a better refinement is required, a linear combination of the polynomials f_i can be considered in addition.

In view of a better understanding of this behavior, the examples developed by the authors relate to the hypotheses of shear undeformability of the mid-surface ("a"), basic shear deformability ("b" – only the average shear strains Γ_x and Γ_y are present), and refined shear deformability ("c" – further terms $\Gamma_i f_i$ are present in addition to Γ_x and Γ_y). In this last case the approximation has been truncated at the second order ($N_o = 2$), thus allowing to use the polynomials indicated in Table 2.

The numerical results have been obtained by using a mesh of 100 two-node finite elements over the beam length. Depending on what approximation is considered ("a", "b" or "c"), the overall degrees of freedom are as indicated in Table 3.

A convergence check has been carried out indicating the high accuracy of the mesh size.

In Table 4 the critical values of the dimensionless transverse force λ_F are presented for different values of the normalized axial compressive force v:

$$\lambda_F = \frac{FL^2}{\sqrt{G_{tz} J_t \cdot D_{zz} I_{yy}}} \tag{78.a}$$

$$v = \frac{P}{\pi^2 D_{zz} I_{yy} / 4L^2} \tag{78.b}$$

As a second goal, the coupling effect between deformability in shear and geometric non-linearity has been investigated. The two following dimensionless quantities are introduced for this scope:

$$\delta(z) = \frac{\eta_c(z)}{\eta_c^*|_{z=L}} \quad \gamma(z) = \frac{\varphi_x(z)}{\varphi_x^*|_{z=L}} \tag{79.a, b}$$

where the symbols $\eta_c^*|_{z=L}$ and $\varphi_x^*|_{z=L}$ denote, respectively, the deflection η_c and the rotation φ_x predicted via a linear analysis without accounting for the shear deformability on the mid-surface.

In Tables 5a and b the numerical predictions in terms of the free end dimensionless deflection and flexural rotation are presented. The results dealing with the models "a", "b" and "c", as well as the different values of the normalized axial force are compared. Both the linear (L) and the non-linear (NL) analysis are considered. It has been also assumed that the external transverse force F corresponds to the lowest value indicated in Table 4 (i.e. model "c").

The investigation is limited to $\alpha = 1$.

Furthermore, the functions $\delta(z)$ and $\gamma(z)$ are plotted in Figs. 6a and b, 7a and b versus the normalized axial coordinate z/L.

As it can be argued from the values presented in Table 4, the refined approach proposed by the authors for modeling the shear deformability (model "c") allows to capture a not negligible reduction of the critical load in respect to the hypothesis of considering zero shear strains along λ ("model "a") or the classical average shear strains ("model "b"). For the less slender beam ($\alpha = 1$) this decrease is found equal to about −15% with respect to model "a"

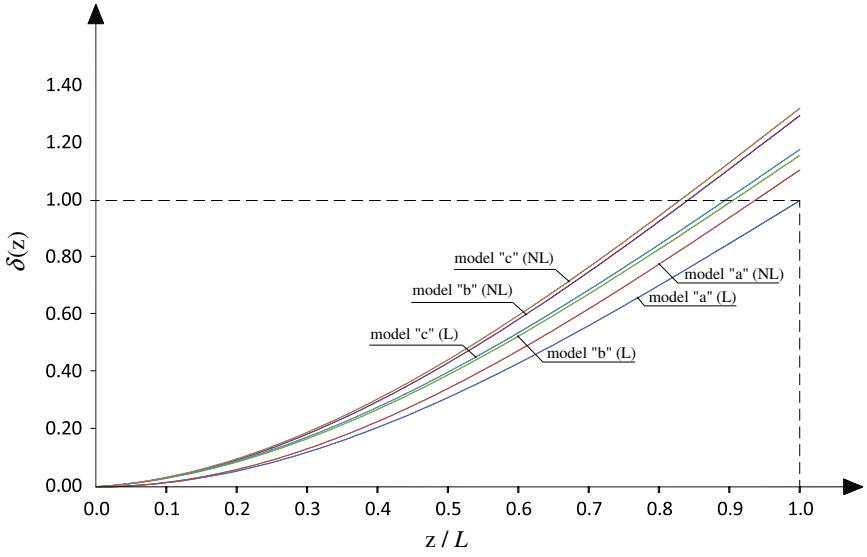

Fig. 6a. Diagram of $\delta(z)$ versus z/L($\alpha = 1$, $v = 0.3$).

Please cite this article in press as: Mancusi G, Feo L. Non-linear pre-buckling behavior of shear deformable thin-walled composite beams with open cross-section. Composites: Part B (2012), http://dx.doi.org/10.1016/j.compositesb.2012.11.003

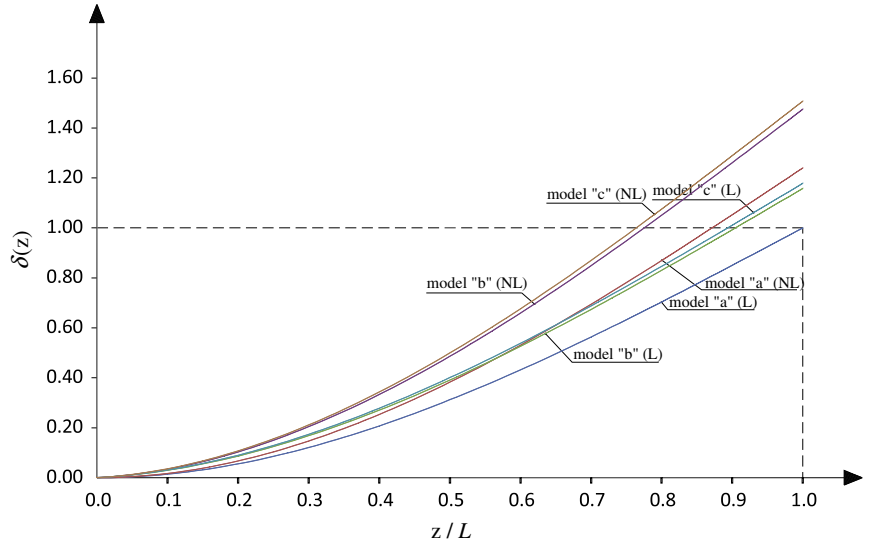

Fig. 6b. Diagram of $\delta(z)$ versus $z/L(\alpha = 1, \nu = 0.6)$.

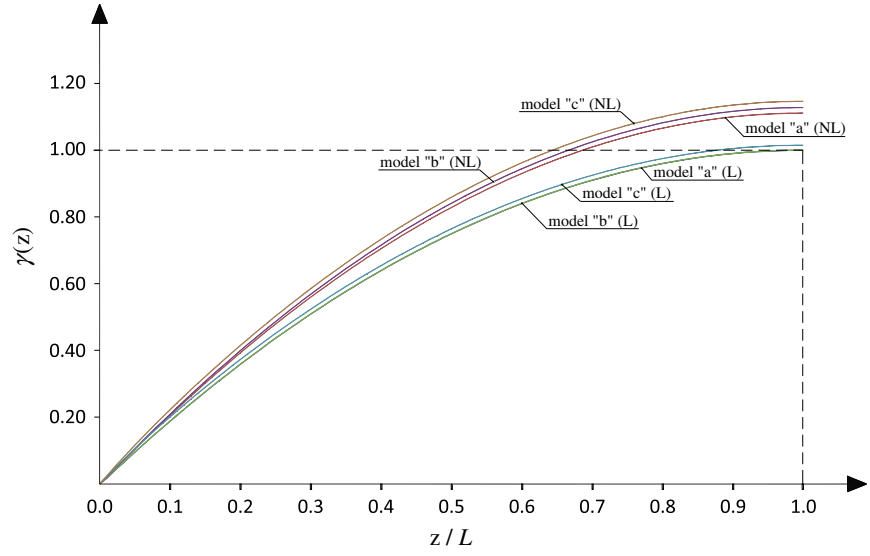

Fig. 7a. Diagram of $\gamma(z)$ versus $z/L(\alpha = 1, \nu = 0.3)$.

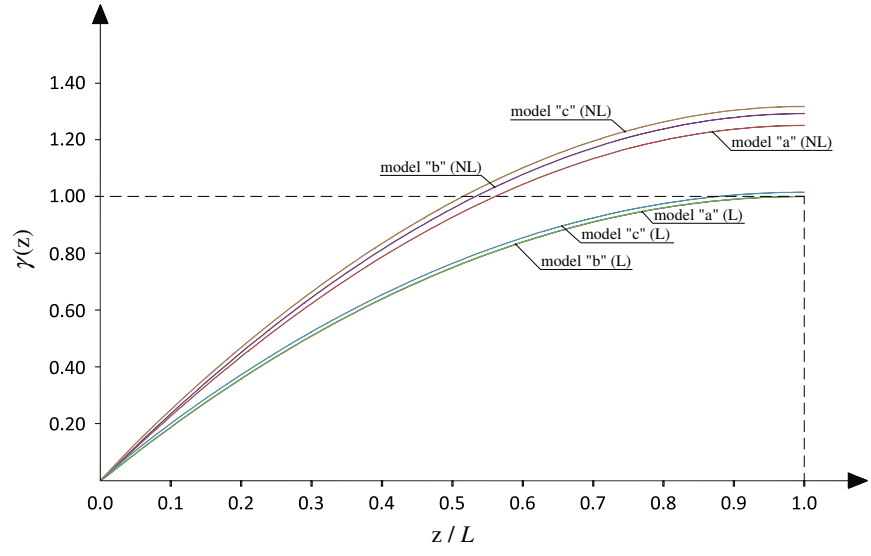

Fig. 7b. Diagram of $\gamma(z)$ versus $z/L(\alpha = 1, \nu = 0.6)$.

Please cite this article in press as: Mancusi G, Feo L. Non-linear pre-buckling behavior of shear deformable thin-walled composite beams with open cross-section. Composites: Part B (2012), http://dx.doi.org/10.1016/j.compositesb.2012.11.003

or equal to about −10% with respect to model "*b*". On the contrary, no relevant differences are found for the analysis relating to the other beam ($\alpha = 5$).

Moreover, in the case $\alpha = 1$, a coupling effect between non linearity and deformability in shear also emerges in terms of free end deflection (Table 5a). Despite the fact that only +17.8% is found via a linear analysis (model "*c*" with respect to model "*a*"), the end deflection increases up to +21.5% (model "*c*" in respect to model "*a*" – $\nu = 0.6$) if a non-linear analysis is carried out.

For what concern the analogous effect relating to the free end rotation (Table 5b), the differences are less relevant between a model and another.

5. Conclusions

In this paper the authors have presented a mechanical model for the study of the non-linear pre-buckling behavior of composite beams with open cross-section.

The model accounts for a refined approximation of the shear deformability on the mid-surface of the walled beam. Geometric non linearity is considered according to the hypotheses of small strains and moderate rotations.

The numerical results have shown a relevant dependency of the mechanical behavior on the shear deformability, both within the linear and the non-linear field. Comparisons in terms of load multipliers indicate that for low slenderness ratios the shear strains can highly affect the buckling load of the pultruded beam.

Flexural deflections and rotations are also influenced in a combined manner by shear deformability and moderate rotations, indicating the need to improve the knowledge and understanding of such an interaction in the perspective of a safe use of composite profiles for civil engineering applications.

References

[1] Vlasov VZ. Thin-walled elastic beams. New York: Pergamon Press; 1961.
[2] Vasiliev VV. Mechanics of composite structures. London: Taylor and Francisr; 1993.
[3] Barbero EJ. Introduction to composite material design. Bristol (PA): Taylor and Francis; 1993.
[4] Piovan MT, Cortı'nez VH. Mechanics of shear deformable thin walled beams made of composite materials. Thin-Wall Struct 2007;45:37–62.
[5] Kim NI, Kim MY. Exact dynamic/static stiffness matrices of non-symmetric thin-walled beams considering coupled shear deformation effects. Thin-Wall Struct 2005;43:701–34.
[6] Ascione L, Feo L, Mancusi G. On the statical behaviour of FRP thin walled beams. Composites Part B 2000;31(8):643–54.
[7] Feo L, Mancusi G. Modeling shear deformability of thin-walled composite beams with open cross-section. Mech Res Commun 2010;37(3):320–5.
[8] Minghini F, Tullini N, Laudiero F. Locking-free finite elements for shear deformable orthotropic thin-walled beams. Int J Numer Meth Eng 2007;72:808–34.
[9] Brooks RJ, Turvey GJ. Lateral buckling of FRP pultruded GRP I-section cantilevers. Compos Struct 1995;32:203–15.
[10] Davalos JF, Qiao P, Salim HA. Flexural–torsional buckling of pultruded fiber reinforced plastic composite I-beams: experimental and analytical evaluations. Comput Struct 1997;38:241–50.
[11] Qiao P, Zou G, Davalos JF. Flexural–torsional buckling of fiber reinforced plastic composite cantilever I-beams. Comput Struct 2003;60:205–17.
[12] Mottram JT, Brown ND, Anderson D. Buckling characteristics of pultruded glass fibre reinforced plastic columns under moment gradient. Thin-Wall Struct 2003;41:619–38.
[13] Kolla' r LP. Flexural–torsional buckling of open section composite columns with shear deformation. Int J Solids Struct 2001;38:7525–41.
[14] Lee J, Kim SE. Flexural–torsional buckling of thin-walled I-section composites. Comput Struct 2001;79:987–95.
[15] Sapka's A', Kolla' r LP. Lateral–torsional buckling of composite beams. Int J Solids Struct 2002;39. 2939–2363.
[16] Lee J, Kim SE, Hong K. Lateral buckling of I-section composite beams. Eng Struct 2002;24:955–64.
[17] Roberts TM. Influence of shear deformation on buckling of pultruded fiber reinforced plastic profiles. J Compos Constr 2002;6:241–8.
[18] De Lorenzis L, La Tegola A. Effect of applied stresses on global buckling of isotropic and transversely isotropic thin-walled members: theoretical analysis. Compos Struct 2005;68:339–48.
[19] Ascione L, Giordano A, Spadea S. Lateral buckling of pultruded FRP beams. Composites Part B 2010;42(4):819–24.
[20] Cortı'nez VH, Piovan MT. Stability of composite thin-walled beams with shear deformability. Comput Struct 2006;84:978–90.
[21] Lin ZM, Polyzois D, Shah A. Stability of thin-walled pultruded structural members by the finite element method. Thin-Wall Struct 1996;24:1–18.
[22] Minghini F, Tullini N, Laudiero F. Buckling analysis of FRP pultruded frames using locking-free finite elements. Thin-Wall Struct 2008;46:223–41.
[23] Naghdi PM, Vongsarnpingoon L. Small strain accompanied by moderate rotation. Arch Ration Mech Anal 1982;80:263–94.
[24] Naghdi PM, Vongsarnpingoon L. Theory of shells with small strain accompanied by moderate rotation. Arch Ration Mech Anal 1983;83:245–83.
[25] Angelillo M. On the characterization of the theory of small strains and moderate rotations to thin bodies, Report no. 196, Istituto di Costruzioni, Facoltà di Architettura, University of Naples; 1988.
[26] Argyris J. An excursion into large rotations. Comput Meth Appl Mech Eng 1982;32:85–155.
[27] Fraternali F, Feo L. On a moderate rotation theory of thin-walled composite beams. Composites: Part B 2000;31:141–58.
[28] Ascione L, Berardi VP, Feo L, Mancusi G. A numerical evaluation of the interlaminar stress state in externally FRP plated RC beams. Composites Part B 2005;36(1):83–90.
[29] Mancusi G, Feo L, Berardi VP. Concrete open-wall systems wrapped with FRP under torsional loads. Materials 2012;5(11):2055–68.
[30] Ascione L, Berardi VP, D'Aponte A. Creep phenomena in FRP materials. Mech Res Commun 2012;43:15–21.
[31] Ascione F, Mancusi G. An experimental analysis on the time-dependent behaviour of a CFRP retrofitting under sustained loads. Proceeding of 6th international conference on fracture mechanics of concrete and concrete structures,catania, Italy, 17–22 June 2007, vol. 2. London (UK): Taylor & Francis; 2007. p. 1085–90.
[32] Mancusi G, Spadea S, Berardi VP, Experimental analysis on the time-dependent bonding of FRP laminates under sustained loads. Composites: Part B 2012. doi:http://dx.doi.org/10.1016/j.compositesb.2012.10.007

Please cite this article in press as: Mancusi G, Feo L. Non-linear pre-buckling behavior of shear deformable thin-walled composite beams with open cross-section. Composites: Part B (2012), http://dx.doi.org/10.1016/j.compositesb.2012.11.003